

We are IntechOpen, the world's leading publisher of Open Access books Built by scientists, for scientists

6,900

Open access books available

186,000

International authors and editors

200M

Downloads

Our authors are among the

154

Countries delivered to

TOP 1%

most cited scientists

12.2%

Contributors from top 500 universities



WEB OF SCIENCE™

Selection of our books indexed in the Book Citation Index
in Web of Science™ Core Collection (BKCI)

Interested in publishing with us?
Contact book.department@intechopen.com

Numbers displayed above are based on latest data collected.
For more information visit www.intechopen.com



Induction Plasma Synthesis of Nanomaterials

Jiayin Guo

Additional information is available at the end of the chapter

<http://dx.doi.org/10.5772/62549>

Abstract

In this chapter, induction plasma technology and its application for synthesis of nanomaterials are introduced. Also, the scientific base for the induction plasma processing of materials is briefly described. Two typical induction plasma systems developed by Tekna for laboratory research and pilot-scale industrial production of nanomaterials, respectively, are presented, together with various examples of the nanopowders, nanotubes, nanorods, and nanowires synthesized using its facilities. The advantages of the induction plasma process over the alternative techniques and its adaptability into industrial-scale operation are particularly illustrated. Some specific issues related to the nanomaterial synthesis process are also discussed.

Keywords: Inductively coupled plasma, synthesis, nanomaterials, nanopowders, nanorods, nanotubes, nanowires

1. Introduction

Nanomaterials have been evolving into a large family including members such as nanoparticles, nanocomposites, nanocapsules, nanoporous materials, nanofibers, nanowires, nanorods, nanotubes, fullerenes, quantum dots, and nanocoatings. Interest in nanomaterials has been continuously increasing in the past decades. Owing to their unusual properties in various aspects such as magnetic, conductive, optical, energetic, and catalytic, nanomaterials are finding more and more industrial applications. [1–5] So far, there are hundreds of types of nanomaterials in use or under development. The market and applications of the nanomaterials can be found in various industries. Examples include inks and pigments, coatings and adhesives in polymers, ultrafine polishing compounds [silicon dioxide (SiO_2) and aluminum oxide (Al_2O_3)], sunscreens and other personal care products [titanium dioxide (TiO_2) and zinc oxide (ZnO)], synthetic bone and tooth materials (calcium and phosphate), life sciences, healthcare and medicines (drug delivery and bioanalysis), aerospace (e.g., lighter and stronger

nanocomposites for weight reduction), defense (solid-fuel rocket propellant, new “thermobaric” bombs, etc.), energy (batteries, fuel cells, solar cells, etc.) [Li_2TiO_3 and silicon (Si)], information technology, telecom and electronics (MLCC) [titanate and nickel (Ni)], automotive and transportation [auto lubricants and copper (Cu)], light-emitting diodes (LEDs; rare earth and nanophosphors), textiles, catalysts, foods and drinks [dietary supplements and silver (Ag)], magnetic separations and MRI contrast agents (iron oxide), 3D printing/additive manufacturing, and so on. It was predicted that by 2017, nanomaterials’ share of the market will have increased to 76.3% on total sales of 37.3 billions.[4] In recent years, 3D printing/additive manufacturing has been developed rapidly. Sales of 3D printing materials are to grow at a compound annual growth rate (CAGR) of 17.9% during the period from 2015 to 2019, reaching at \$650 millions in 2019.[5] The continuously increased demand for nanomaterials stimulated the extensive research and development (R&D) of various techniques and processes,[6] among them thermal plasma being one of the most widely used techniques.

While different techniques and processes have their own features, they all face the same challenges on the road to commercialization, that is, productivity, quality controllability, and affordability. Induction plasma technology used as one of the alternatives for nanomaterial preparation stands out owing to its numerous unique advantages. It has a large-volume, high-temperature plasma zone. It allows for central injection of feed stock, making possible in-flight evaporation of even the highest boiling-point raw materials. It can be operated under various atmospheres, permitting synthesis of various nanomaterials. Due to the extensive R&D in the last two decades, induction plasma process has become a much more reliable and efficient technology than ever, making it suitable for preparation of nanomaterials in both laboratory and industrial scales. Indeed, induction plasma technology used for synthesis of nanomaterials has gained increased popularity around the world in recent years,[6–39] thanks to a great extent to the availability and improvement of the technology itself.

Boron nitride nanotube (BNNT), due to its potential superior properties over carbon nanotube, has attracted people’s interests since its discovery in 1995.[40–47] This material was synthesized using arc discharge between a BN-packed tungsten (W) rod and a cooled Cu electrode[40] and laser ablation technique under high pressure.[44] However, these techniques resulted in very low productivity of less than a few grams per hour. It was recently demonstrated that induction plasma process can be conveniently used to produce BNNT at large quantity (>180 g/day).[45]

2. Theoretical

2.1. Induction plasma generation and its properties

Induction plasma is generated through induction coupling mechanism. When an alternative current of radio frequency and high voltage is imposed on a spiral coil, the conductor placed in the center of the coil will be heated up under the alternative electromagnetic field. Introducing a continuum gas flow into such coil could heat the gas and ionize it into plasma. The plasma so generated is called inductively coupled plasma or induction plasma in short. Figure

1(a) and (b) shows the mechanism of induction plasma torch and the photo of induction plasma generated by high-frequency discharge, respectively.

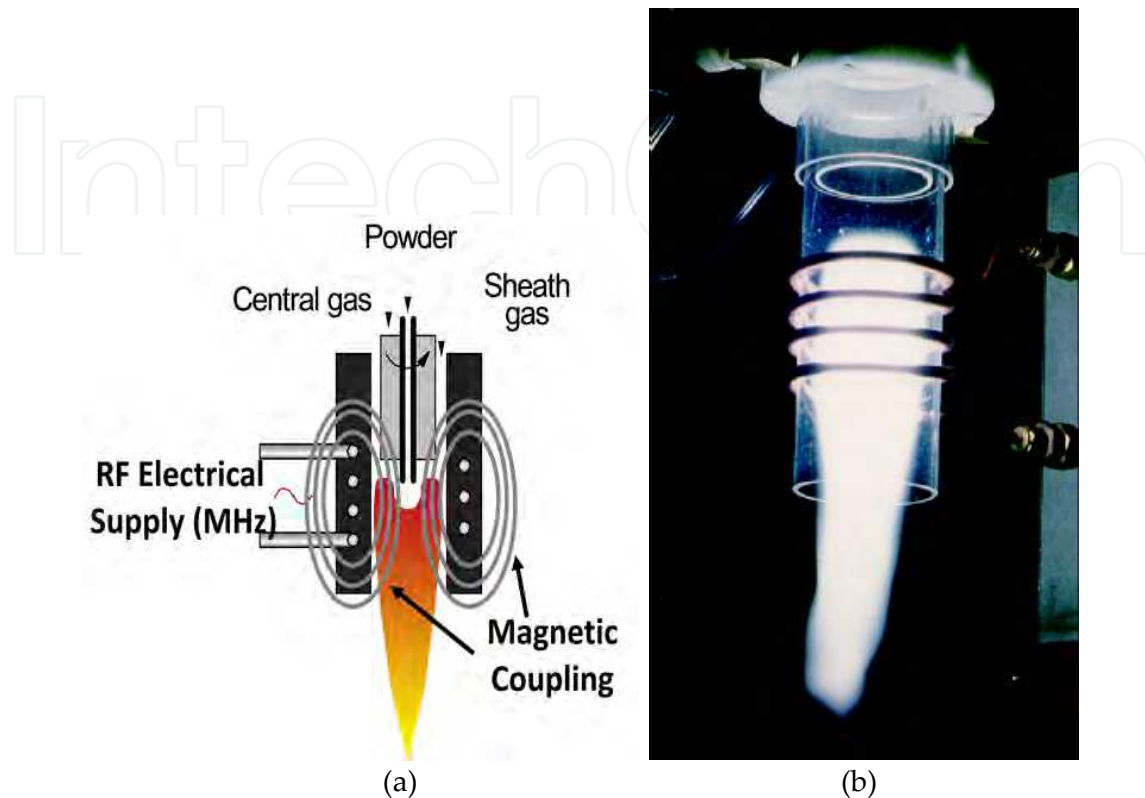


Figure 1. (a) Schematic of the mechanism of induction plasma torch (b) Photo of induction plasma generated by high frequency discharge

Tekna has been the world leader in the induction plasma technology. Its proprietary plasma torches have been widely used in numerous research laboratories and industrial R&D centers, as shown in Figure 2(a) and (b). They are featured by following characteristics: (1) ceramic tube used to confine plasma providing a high-purity processing environment; (2) solid torch body encapsulating the induction coil, which eases the manipulation during maintenance and certifies a perfect positioning of the coil during assembly; (3) easily interchangeable nozzle design allowing for replacement of nozzles of various diameters and configurations; and (4) variable position of the central injection probe for optimum performance based on process needs. Tekna has developed different models of plasma torches to match different power supplies of various frequency and power level requirements (see Table 1).

Induction plasma process has numerous advantageous characteristics. It is electrodeless and thus has no issue of erosion-caused contamination. As a clean heat source, it is particularly suitable for high-purity material processing. Because of its relatively large volume of high temperature zone and low gas velocity, induction plasma is an ideal tool for high-temperature material processing where melting or evaporation of material is required. Induction plasma is not only a heat source but can be a chemical reaction source as well due to the fact that almost

any kinds of gases (Ar, He, H₂, O₂, N₂, air, NH₃, CH₄, or mixtures) can be used as the plasma working gas.

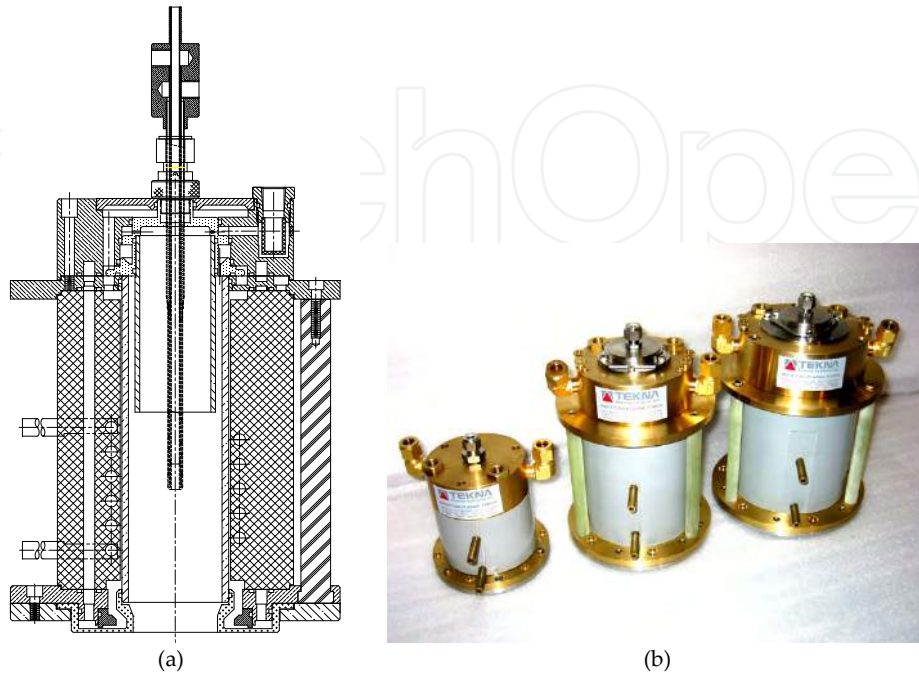


Figure 2. (a) Tekna's ceramic wall plasma torch design (U.S. Patent #5200595 and International PCT/CA92/00156) (b) Tekna's plasma torches used for different power levels

Torch	Frequency	Power (kW)
PL-25	4-5 MHz	15
PL-35	2-4 MHz	30
PL-50	2-4 MHz	60
PL-70	400 kHz-4 MHz	100
PL-100	400 kHz-4 MHz	200-500

Table 1. Tekna's induction plasma torch series

In an induction plasma torch, the highest temperatures always occur away from the axis. This is caused by the skin effect existing in high-frequency electromagnetic field. However, the skin depth is an important parameter in determining the coupling efficiency of the induction plasma torch. The skin depth can be expressed as follows:

$$\text{Skin depth } \delta = \frac{1}{\sqrt{\pi \xi_0 \sigma f}},$$

where $\xi_0 = 4\pi \times 10^{-7}$ (H/m or Vs/Am) is the magnetic conductivity under vacuum; σ is the electrical conductivity of the load (mho/m or A/Vm) ($\sigma = 1000$ S/m for Ar plasma, corresponding to about 8000 K); f is the working frequency (Hz or s^{-1}). If $f = 3$ MHz, then the skin depth $\delta = 9$ mm. An illustration of the skin depth in an induction plasma torch is shown in Figure 3.

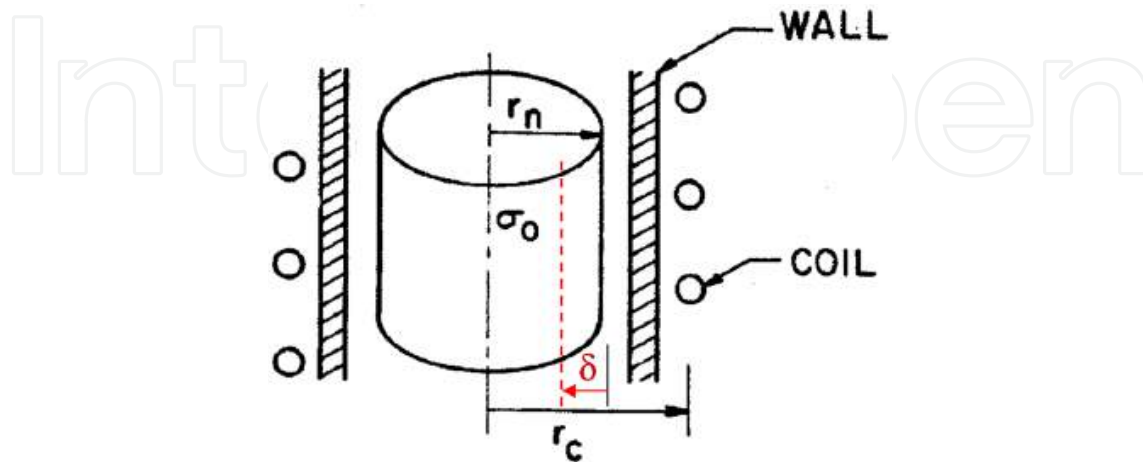


Figure 3. Illustration of the skin depth in an induction plasma torch

Based on the modeling and experimental results of a standard PL-50 plasma torch,[48] the typical velocity of plasma/particle in the torch is 20–80 m/s, and the resultant typical residence time of particles in the plasma is about 0.5–2 ms.

To make better use of the limited residence time and to increase the heating rates of the particles injected into the plasma, one should increase the enthalpy and thermal conductivity of the plasma, which can usually be achieved by changing the plasma gas compositions. The enthalpies of some of the most common plasma gases (H_2 , N_2 , O_2 , He, Ar) as a function of temperature are shown in Figure 4, where, in general, hydrogen plasma has the highest enthalpy ($350\text{--}450$ kJ/kg $\times 10^3$ in the range of 6000–10,000 K), whereas the argon plasma has the lowest ($2\text{--}5$ kJ/kg $\times 10^3$ for the same temperature range). Figures 5 and 6 show the thermal conductivity of pure nitrogen plasma and ($Ar + H_2$) mixture plasma as a function of temperature, respectively. As shown in Fig. 6, pure argon has poor thermal conductivity in the working temperature range, but addition of hydrogen can significantly increase the thermal conductivity of ($Ar + H_2$) mixture plasma. The occurrence of peak values in thermal conductivity for both Figures 5 and 6 is due to the contribution of dissociation of molecules to atoms ($N_2 \rightarrow N$ or $H_2 \rightarrow H$) or ionization of atoms to ions ($N \rightarrow N^+$ or $H \rightarrow H^+$).

2.2. Induction plasma used for nanomaterial synthesis

Synthesis of nanomaterials in induction plasma is accomplished by either pure physical process or chemical process. The physical process is an evaporation–condensation process, in which the material is first heated up and evaporated in the plasma, and the resulting vapors are subsequently subjected to a very rapid quench where homogeneous nucleation gives rise to the formation of nanoparticles. The chemical process refers to any synthesis route where

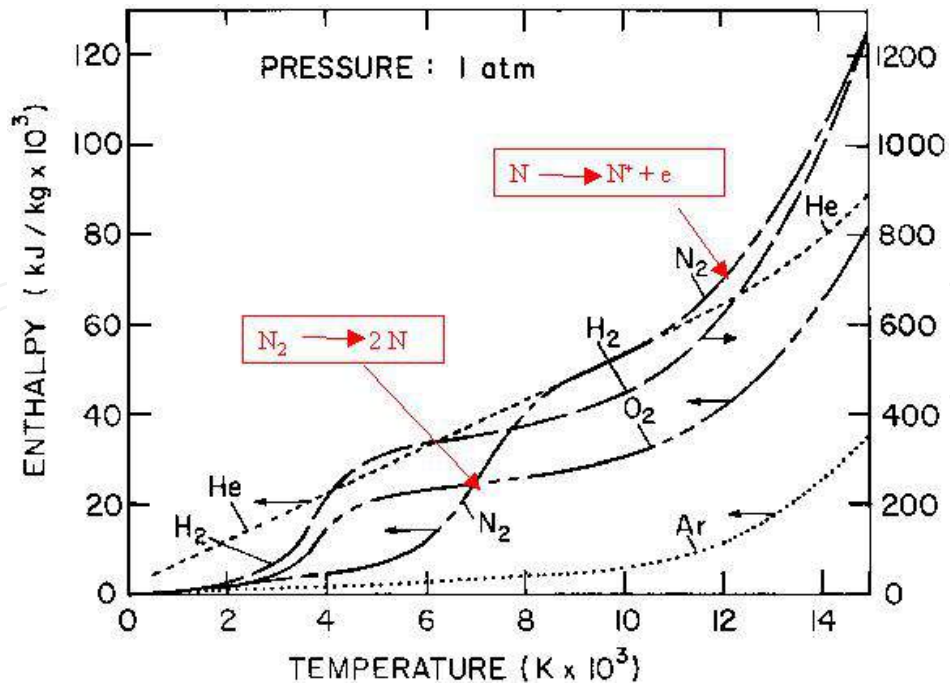


Figure 4. Specific enthalpy of various gases as a function of temperature (at atmospheric pressure) [6, 49].

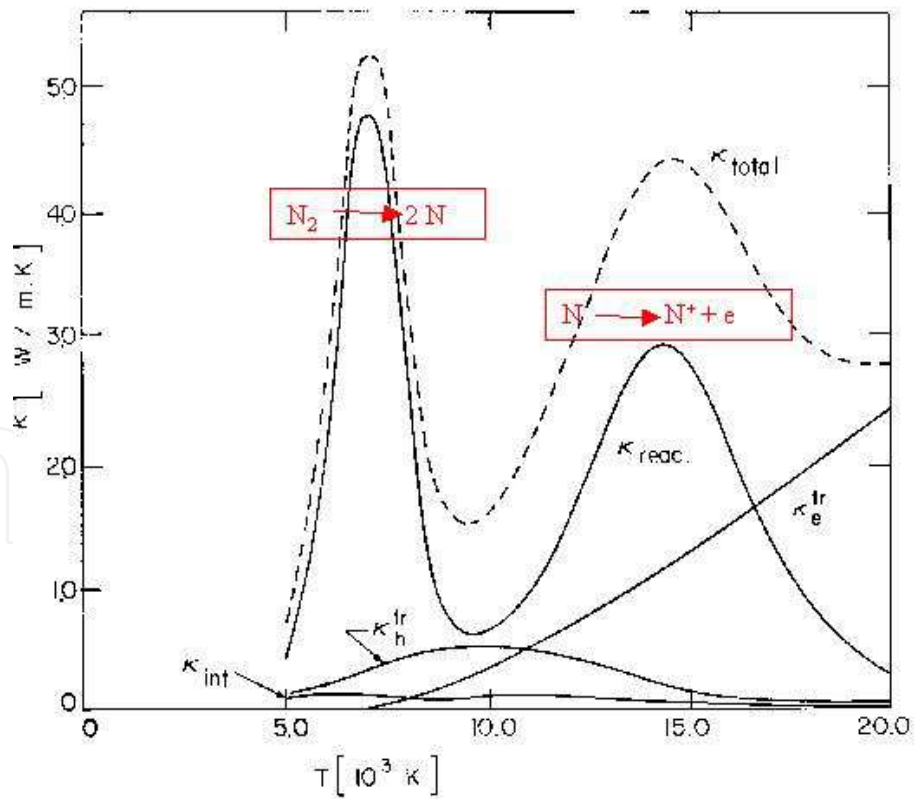


Figure 5. Thermal conductivity of nitrogen as a function of temperature (at atmospheric pressure) [6, 49].

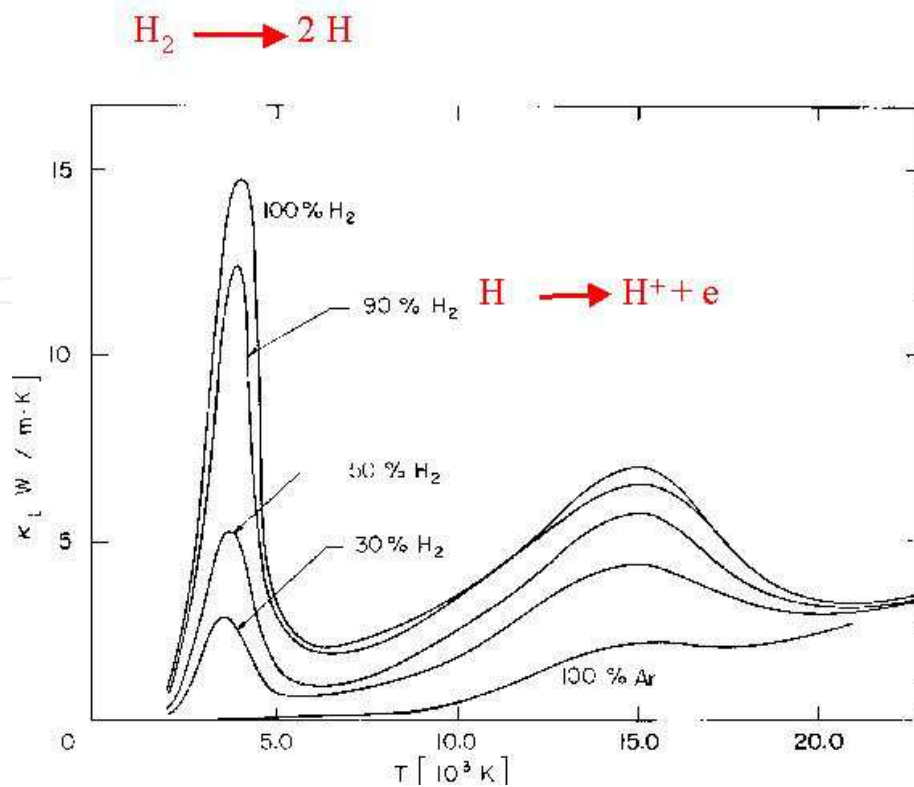


Figure 6. Thermal conductivity of (Ar+H₂) mixture as a function of temperature (at atmospheric pressure) [6, 49].

chemical reaction is involved. It is an evaporation–reaction–condensation process, in which one or more gaseous reactants react with the vapor generated from the material introduced into the plasma reactor, and the resultant product condenses to form nanoparticles. The gaseous reactant can be a plasma gas component or separately injected at appropriate locations (into the plasma zone or in the reactor). Nanomaterial syntheses through thermal decompositions and pyrolysis of the precursors in the plasma followed by condensation are also included in the chemical processes. The quench agent used can be inert gases such as Ar and N₂ or reactive gases such as CO₂, CH₄, and NH₃, depending on the needs of the process and the type of the nanomaterial to be synthesized. Based on the modeling results by Guo et al., [6] gas quench rate achievable in a typical plasma reactor is in the order of magnitude of 10⁶ K/s. Porous filters (metallic or polymeric) are usually used for collection of the nanomaterials prepared, which are installed downstream from the plasma reactor section. In the case of synthesis of metallic or other reactive powders, special care should be taken to powder handling and manipulation. Usually, passivation of the powders is required prior to their removal from the filtration section of the process or from a glove box.

Figure 7 illustrates the process steps of nanomaterials' synthesis in induction plasma. The in-flight vaporization of the feed material is a prerequisite for synthesis of uniform nanomaterials. The fed particle gets heat from plasma through convection heat transfer and internal conduction while it loses heat to environment through radiation. To ensure the vaporization of the particle, the total net heat it absorbs has to be greater than the sum of the heat it needs to be

heated up to vaporization point and its latent heats of melting and vaporization. A heat balance analysis for in-flight plasma vaporization of fed powders is illustrated in Figure 8.

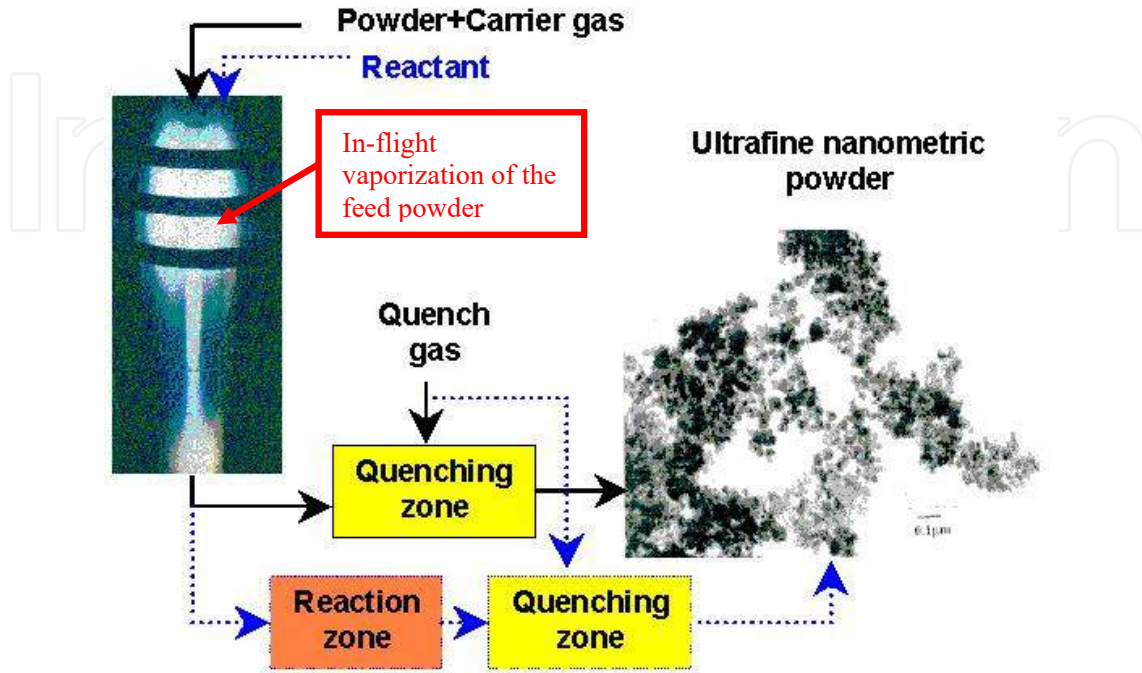


Figure 7. Illustration of nanopowder formation in RF plasma through two different routes.

In-flight Melting and VAPORIZATION of Powders

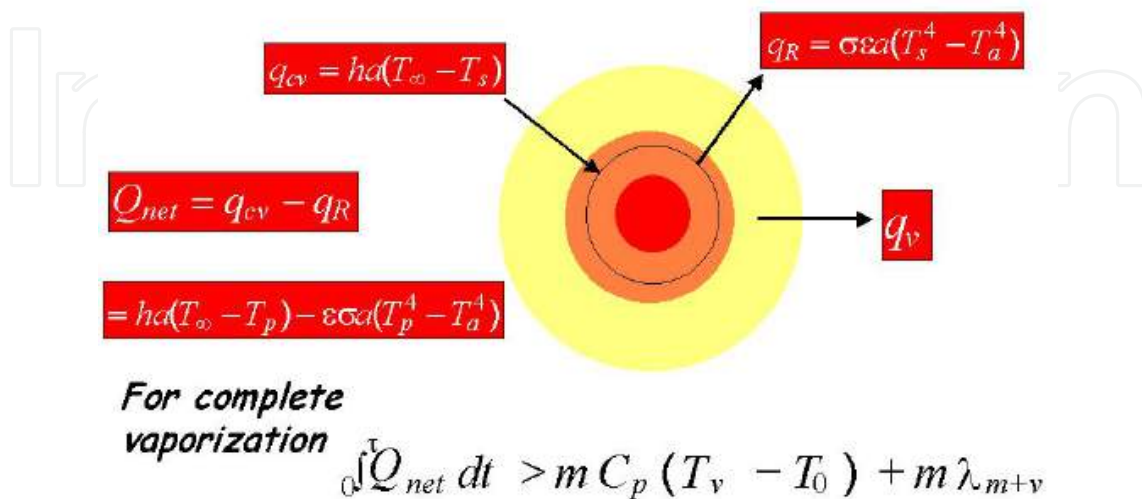


Figure 8. An analysis of thermal balance for in-flight plasma vaporization of fed powders.

Table 2 lists out a detailed overall comparison of the induction plasma to the alternative techniques used for synthesis of nanomaterials.

	Wet Process (Sol-gel)	Ball Milling	Lasers	DC Plasma	Induction Plasma
Technology principle	Wet chemistry. Powder produced through precipitation from an aqueous solution.	Powder produced through the crushing of the material in a high intensity ball mill	Flash evaporation of the precursor using a laser beam followed by the rapid quench of the vapor	Evaporation / condensation process based on either in-flight or pool melting and evaporation	Strictly In-flight evaporation and condensation. Can be used with solid, liquid or gaseous precursors
Powder quality	High purity but agglomerated. Non spherical and poor crystallinity	Limited purity and uniformity of the composition	High purity and quality of the powder	Limited purity, highly agglomerated	High purity, spherical particles with soft agglomeration
Flexibility / limitation	Limited to oxide ceramics; Lengthy post treatment (filtration, drying, de-agglomeration, etc.)	Impurities pick-up; Limited type of powders (metallic)	Limited to low production capacity ; Precursor selectivity	Limited by the small volume of the discharge; Presence of electrodes	Highly flexible applicable to a wide range of metallic and ceramic materials.
Process	Continuous	Batch	continuous	Continuous	Continuous, scalable
Cost	Low cost	Low cost	High cost	Mid cost	Mid cost

Table 2. Comparison of various techniques for nanomaterial synthesis

3. Experimental

3.1. Resume of the nanomaterials synthesized using induction plasma system

Over the past two decades or so, Tekna has been actively involved in R&D of the nanomaterial synthesis using induction plasma technology. It has developed turnkey systems used for both laboratory-scale and pilot-scale production of various nanomaterials. A typical plasma material processing system is composed of the following sections: (1) feedstock preparation and injection; (2) evaporation/reaction; (3) quench; (4) powder collection; and (5) process control. Figure 9 shows schematically a pilot-scale 60 kW induction plasma reactor set-up used for nanomaterial synthesis at Tekna, which is featured by full automation, flexible operation, gas recycling, and powder handling in glove box. Figure 10 shows a complete laboratory-scale 15 kW induction plasma system, which is a compact design and used essentially for production of small samples in research projects. The typical size of the nanoparticles produced ranges from 15 to 200 nm, depending on the material type and operating conditions employed. A summary on the nanomaterials synthesized at Tekna's systems is detailed in Table 3. The list

of materials is getting longer as more activities are carried out to meet the increased demands from the market.

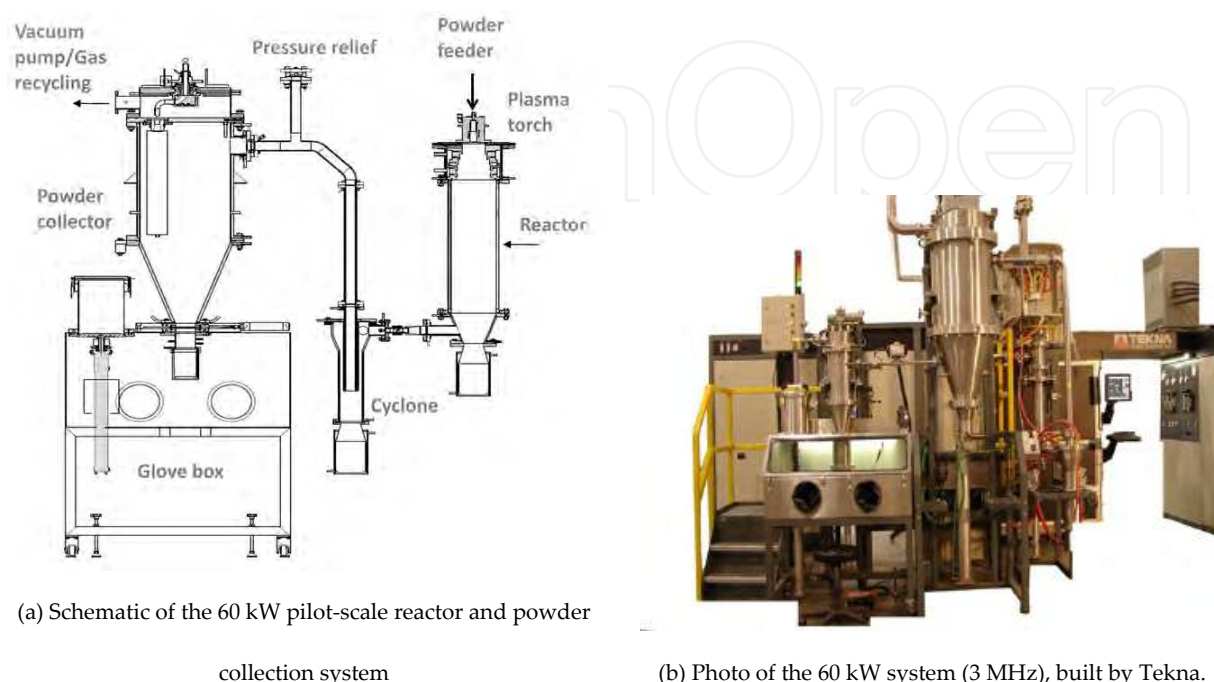


Figure 9. Tek60 Nano - 60 kW pilot-scale RF induction plasma set-up used for nanomaterial synthesis at Tekna

3.2. Synthesis of pure metals and alloys (Al, Cu, Ag, Ni, Fe, Co, Cr, Si, B, Mo, Ta, W, Re, etc.)

Nanosized metal or alloy powders have been prepared through pure evaporation–condensation manner. Coarse particles of pure metal or alloy are injected into induction plasma torch for vaporization and recondensation. The particle sizes and distributions of the feedstock ought to be carefully selected to obtain the optimal results of the nanomaterials synthesized. An alternative route used often for synthesis of pure metal powders is to go through pyrolysis or decomposition of metal-containing precursors in induction plasma.

Figure 11 shows the characteristics of the nanosized aluminum (Al), Ni, Ag, Cu, Si, chromium (Cr), boron (B), molybdenum (Mo), and tungsten (W) powders. In the case of Ni, it was also synthesized from the decomposition of nickel carbonyl ($\text{Ni}(\text{CO})_4$) in plasma (Figure 11(b-2)). These examples represent the group of materials with low boiling points ($<2600^\circ\text{C}$), medium boiling points ($2600\text{--}4000^\circ\text{C}$), and high boiling points ($4000\text{--}6000^\circ\text{C}$), respectively. In general, metallic nanoparticles appear spherical while it is also common that some particles have polyhedron shapes as their sizes are reduced, as revealed by the high-magnification field emission scanning electron microscope (FE-SEM) pictures of Ni, B, and Mo in Figure 11(b-1), (g), and (h-2), respectively.

Fine metallic powders can be highly pyrophoric, handling and storage of such powders are, therefore, of great concern to users. The passivation of the particle surface is a very important task during the preparation of the nanometric metal powders. The passivation can be performed in dry conditions, such as controlled oxidation with air, or in wet conditions, such as immersion in liquid. Other sophisticated passivation methods include polymer coating, surface carburation, and nitridation.



Figure 10. View of Tek15 Nano – 15 kW laboratory-scale system for nanomaterial synthesis

Type of powders	Examples	Precursors	Mean size, d_p (nm)
Pure metals	Al, Cu, Ag, Ni, Fe, Co, Cr, Mo, Ta, W, Re, Si, B	Solid/gas phases	15 - 200
Alloys/Composites	Al-Mg, Co-Cr, Si-Sn, Si-Zn, Co-Cr ₂ O ₃ , Co-SiO ₂ , Co-TiO ₂	Solid/gas phases	15 - 200
Carbides	SiC, B ₄ C, Mo ₂ C, WC, TaC....	Solid/liquid/gas phases	30 - 100
Nitrides	Si ₃ N ₄ , AlN, BN	Solid/liquid/gas phases	30 - 100
Oxides	CuO, Al ₂ O ₃ , MoO ₃ , TiO ₂ , GeO ₂ , CeO ₂ , Y ₂ O ₃ , SiO, SiO ₂ , In ₂ O ₃ -SnO ₂ (ITO), ZnO, ZrO ₂ +La ₂ O ₃ +Al ₂ O ₃ , Nano-glasses	Solid/liquid/gas phases	20 - 200
Others	C-nanotubes, BN nanotubes, ZnS, ZnO nanorods, Si nanowires	Solid/gas phases	

Table 3. Summary of nanomaterials synthesized using Tekna's induction plasma systems

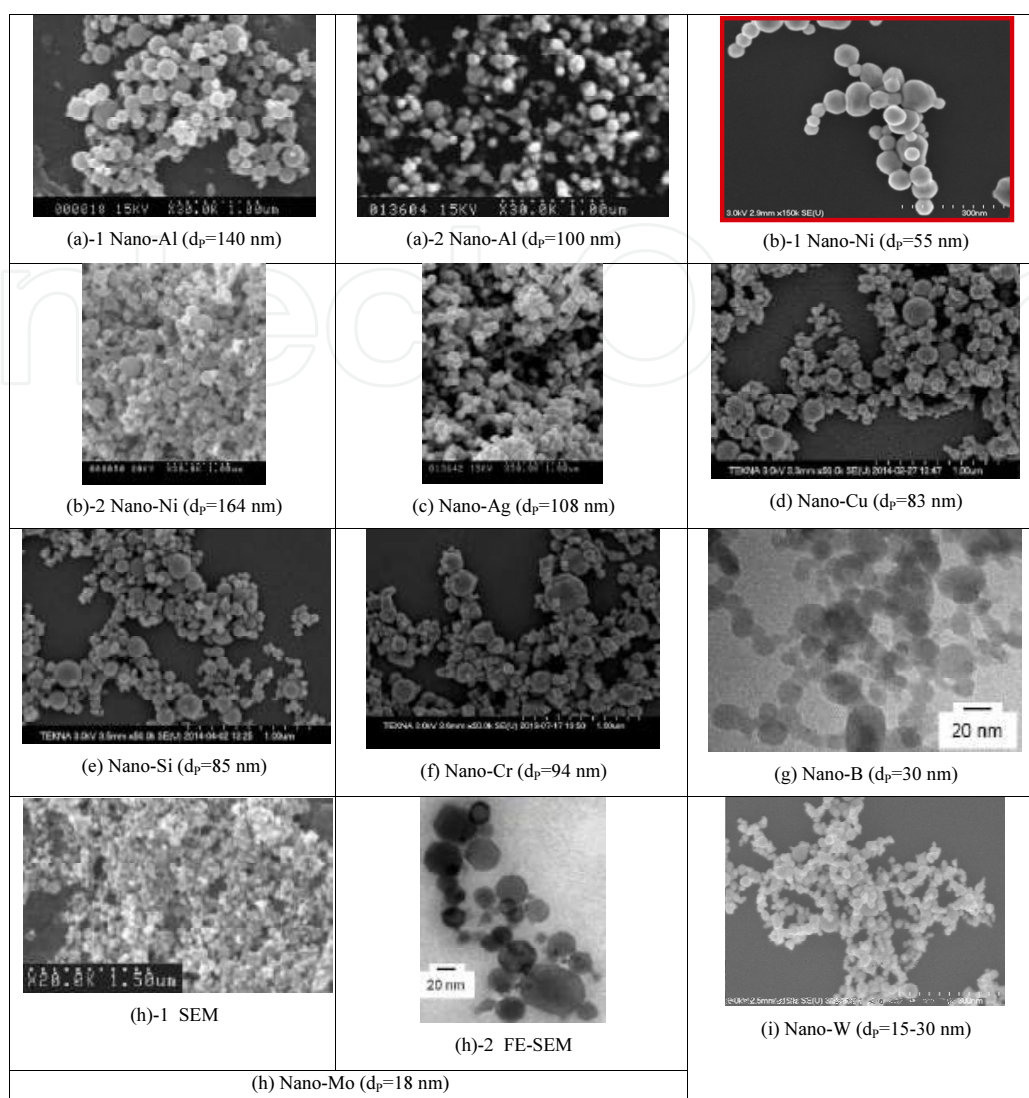


Figure 11. Examples of nanometric metallic powders synthesized [50-66]

3.3. Synthesis of oxides and composites (CuO , Al_2O_3 , MoO_3 , TiO_2 , GeO_2 , CeO_2 , Y_2O_3 , SiO , SiO_2 , SnO_2 , In_2O_3 - SnO_2 (ITO), ZnO , $\text{ZrO}_2 + \text{La}_2\text{O}_3 + \text{Al}_2\text{O}_3$, ZrO_2 , $\text{Gd}_2\text{O}_3 \cdot 2\text{ZrO}_2$, nanoglasses, etc.)

Nanometric oxide powders can be synthesized from oxidation of pure metal or pyrolysis of selected compound (gaseous, liquid, or solid) in induction plasma. In either case, the result depends on the prior evaporation of the injected starting materials, followed by oxidation of the metal vapor by plasma gas (air or oxygen) and condensation of the vapor phase. As mentioned earlier, induction plasma can be operated under different atmospheres. Using oxygen as working gas in induction plasma torch is a convenient choice. It should be mentioned that the oxidation reaction could be highly exothermic. The heat generated could help in evaporation of the feedstock on one hand, but it can also cause reactor temperature rise on the other hand. Thus, extra quench capacity may be required to control the particle sizes and

to avoid agglomeration of the nanopowders produced. Another approach for synthesis of nano-oxide powders is to evaporate the coarse feedstock of same composition in oxygen plasma followed by recondensation. This route could, however, be more challenging because of the high demand of energy intensity and the difficulty of maintaining chemical composition for some materials. The stoichiometry of the product powders obtained could be different from the starting materials after the plasma vaporization and recondensation process.

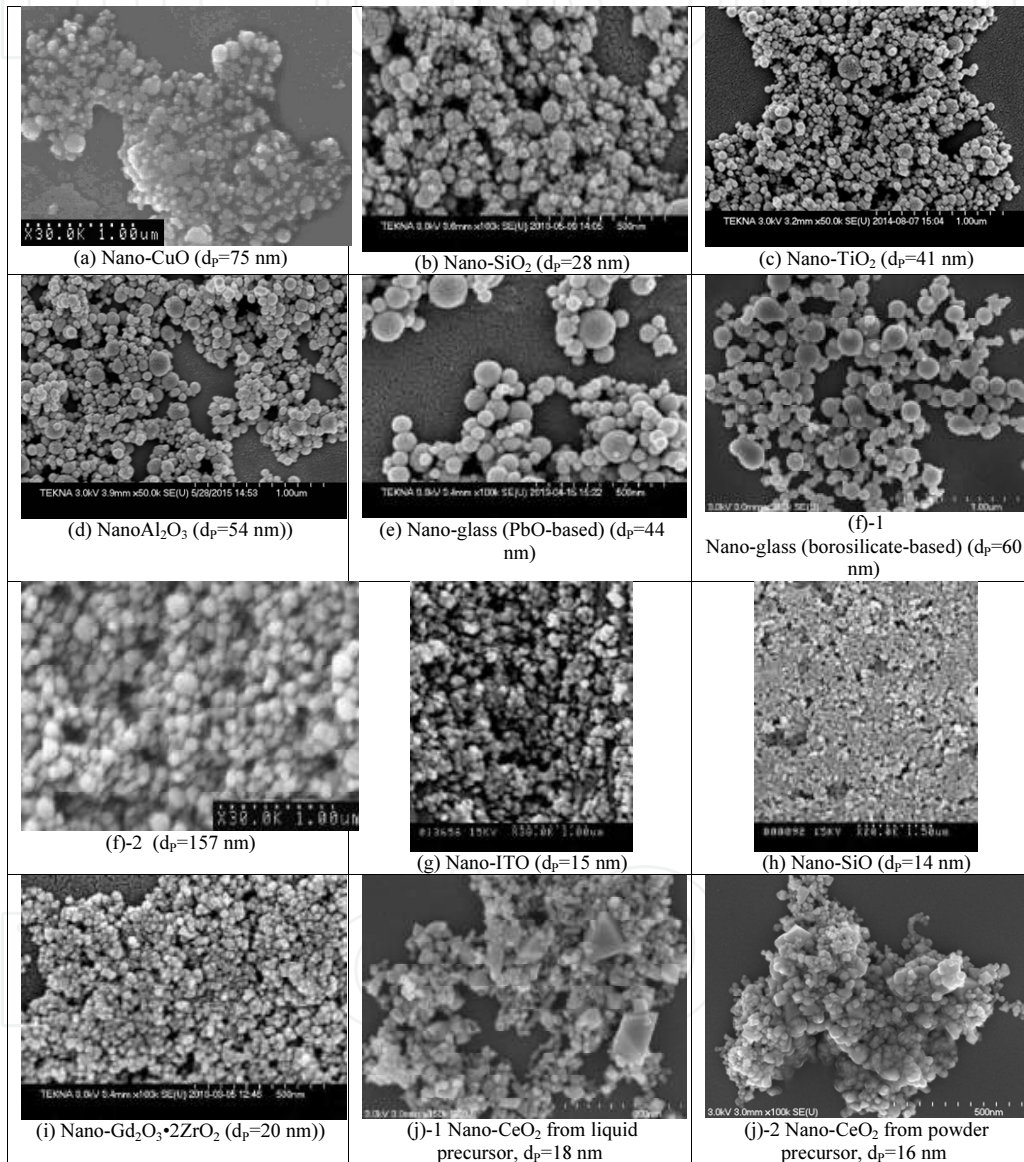


Figure 12. Examples of nanometric oxide powders synthesized [67-89]

Some of the examples of the synthesized nano-oxide powders are shown in Figure 12(a-j), respectively, which are nanosized copper oxide (CuO), SiO₂, TiO₂, Al₂O₃, nanoglass (PbO-based), nanoglass (borosilicate-based), indium tin oxide (ITO), silicon monoxide (SiO),

gadolinium zirconate ($\text{Gd}_2\text{O}_3 \cdot 2\text{ZrO}_2$), and ceria (CeO_2) powders. These powders were synthesized using Tekna's 60 kW system. The CuO , SiO_2 , TiO_2 , and Al_2O_3 powders were synthesized from the reaction of Cu, Si, titanium (Ti), and Al with oxygen in plasma, respectively. In the case of CuO , study was made how to ensure the full oxidation of the injected Cu particles in oxygen plasma. Cu has two states of oxidation, i.e., tenorite (CuO) and cuprite (Cu_2O). It was found that to convert the pure Cu into tenorite, two major parameters had to be well controlled, i.e., oxygen concentration in plasma and the temperature in the reactor.

The nanoglass powders and nano-ITO were synthesized from the evaporation and condensation of coarse feedstock powders in oxygen plasma. By controlling the operating conditions, nanosized glass powders of mean sizes of 44 nm and 157 nm were obtained (Figure 12(f-1) and (f-2), respectively). Nano- SiO particles were synthesized through controlled reduction of SiO_2 powders in induction plasma. Gadolinium zirconate ($\text{Gd}_2\text{O}_3 \cdot 2\text{ZrO}_2$) nanopowders were synthesized from the co-injection of gadolinium- and zirconium-containing precursors into oxygen plasma. The CeO_2 powders were synthesized from two different types of precursors in oxygen plasma. One was a solid precursor, whereas the other was a liquid precursor. In both cases, single-phase CeO_2 were obtained with the mean particle sizes of less than 20 nm.

3.4. Synthesis of advanced non-oxide ceramics (SiC , Si_3N_4 , B_4C , BN , AlN , TiN , WC , TaC , ZnS , etc.)

Non-oxide ceramics are mostly synthesized through chemical reaction in a plasma reactor. Gaseous or liquid organic precursors are often used together with carburetion or nitridation agents for synthesis of non-oxide nanomaterials such as silicon carbide (SiC), silicon nitride (Si_3N_4), aluminum nitride (AlN), titanium nitride (TiN), and boron nitride (BN) through vapor-phase reaction in induction plasma. Examples include synthesis of nano- SiC from injection of silane and methane ($\text{SiH}_4 + \text{CH}_4$) or methyltrichlorosilane (CH_3SiCl_3) into plasma and synthesis of nano- Si_3N_4 from injection of silane and ammonia ($\text{SiH}_4 + \text{NH}_3$) into plasma. Solid precursors can also be used for synthesizing non-oxide ceramic powders in induction plasma reactor, carburetion of Si powder for SiC , and nitridation of Al powder for AlN , for instance. Pure physical process of evaporation–condensation can be used as well for producing some types of ceramic powders that have stable melting and boiling temperatures such as boron carbide (B_4C). It should be pointed out, however, that the evaporation of non-oxide materials often requires very high energy density and long residence time, and, thus, the powder productivity will be very limited. As examples, Figure 13(a-1) and (a-2) shows the micrographs of the nano- SiC synthesized from co-injection of ($\text{Si} + \text{CH}_4$) into induction plasma torch; Figure 13(b) shows the nano- ZnS particles from evaporation and recondensation of the coarse ZnS powders in plasma; Figure 13(c-1) and (c-2) shows nanosized B_4C powders synthesized from solid and liquid precursors, respectively, at Tekna's 60 kW induction plasma unit. X-ray diffraction (XRD) and chemical analyses reveal that these powders consist of predominant B_4C along with some free B and C.

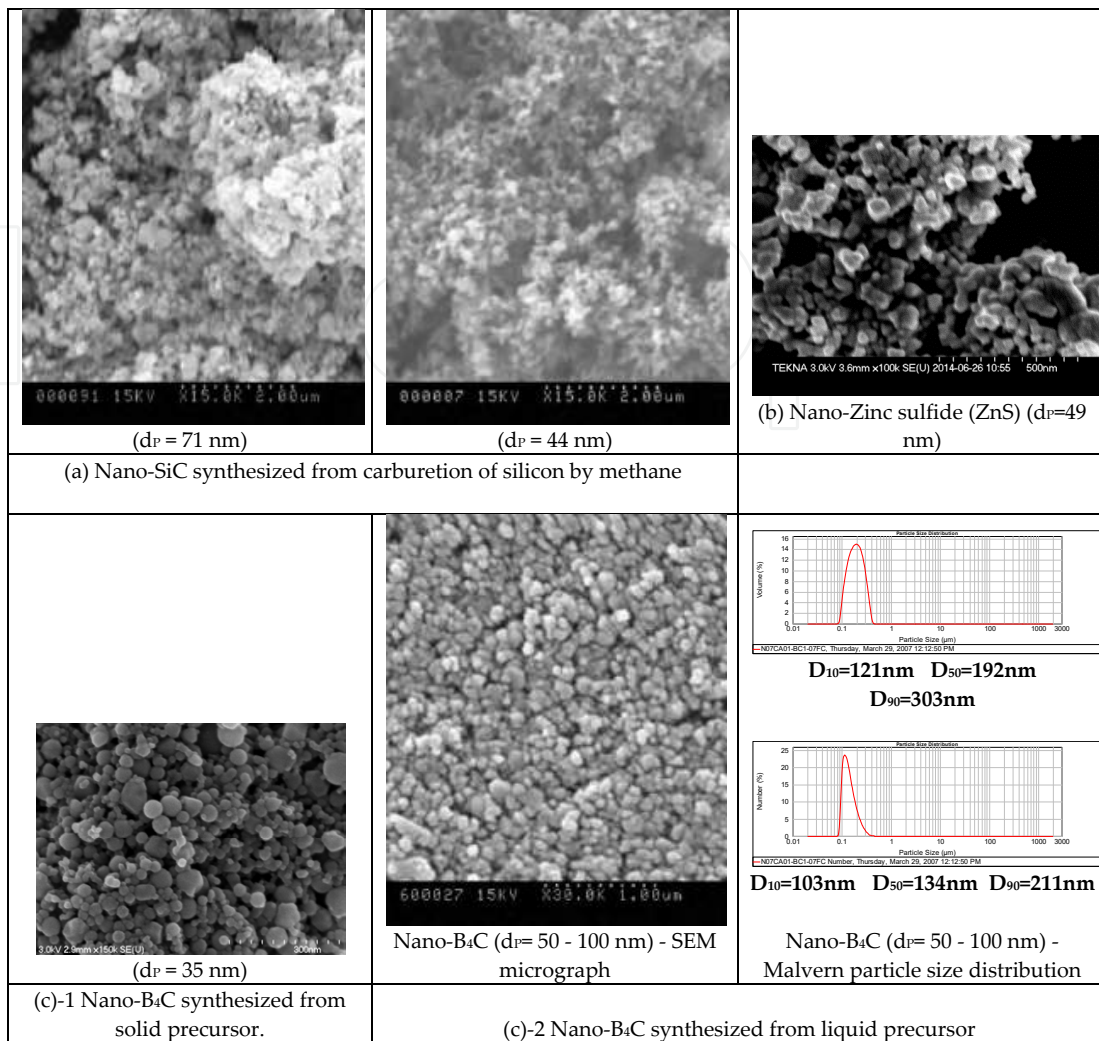


Figure 13. Example of nanometric non-oxide ceramic powders synthesized [90-94]

3.5. Synthesis of other advanced nanomaterials (CNT, BNNT, ZnO nanorods, Si nanowires, etc.)

Induction plasma processes have been successfully used for synthesis of carbon nanotubes, BNNTs, nanorods, and nanowires. Figure 14(a) shows the micrograph of zinc oxide nanorods synthesized from decomposition of zinc-containing compound in oxygen plasma at Tekna's 15 kW unit. Figure 14(b) and (c) shows the micrographs of SiO and Si nanowires, respectively, synthesized at the 15 kW and 60 kW plasma unit. They were obtained by injection of coarse SiO or Si powders into hydrogen or neutral plasma under carefully controlled operating conditions. Figure 14(d) and (e) shows the carbon nanotubes synthesized from different carbon-containing precursors in hydrogen plasma at Tekna and by NRC, respectively. The BNNTs can be synthesized from injection of hexagonal BN powders into induction plasma under a wide range of operating conditions. Figure 14(f) and (g) shows some of the BNNT results obtained.

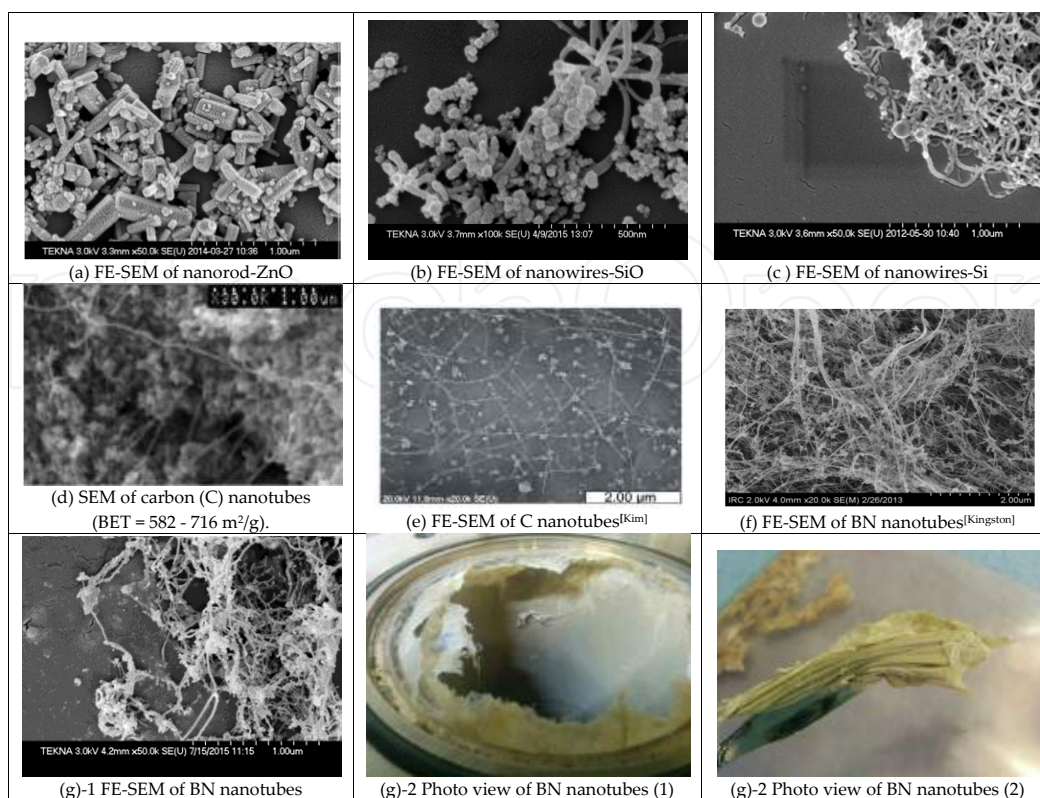


Figure 14. Example of nano-rods, nano-tubes, and nano-wires synthesized using both 15 kW and 60 kW plasma units [64, 73,96, 61, 95, 27-30, 45, 47]

All of these above-mentioned results indicate that induction plasma can indeed be a promising tool for synthesis of various nanomaterials.

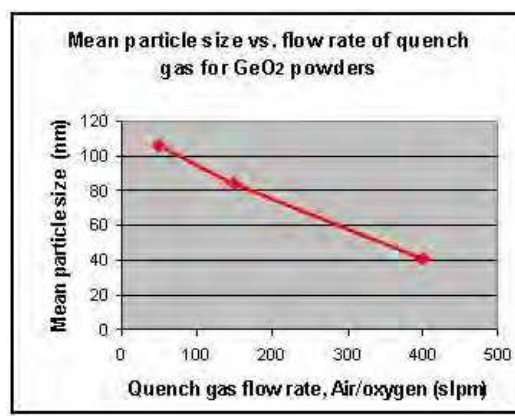
4. Discussion

4.1. Particle size and distribution

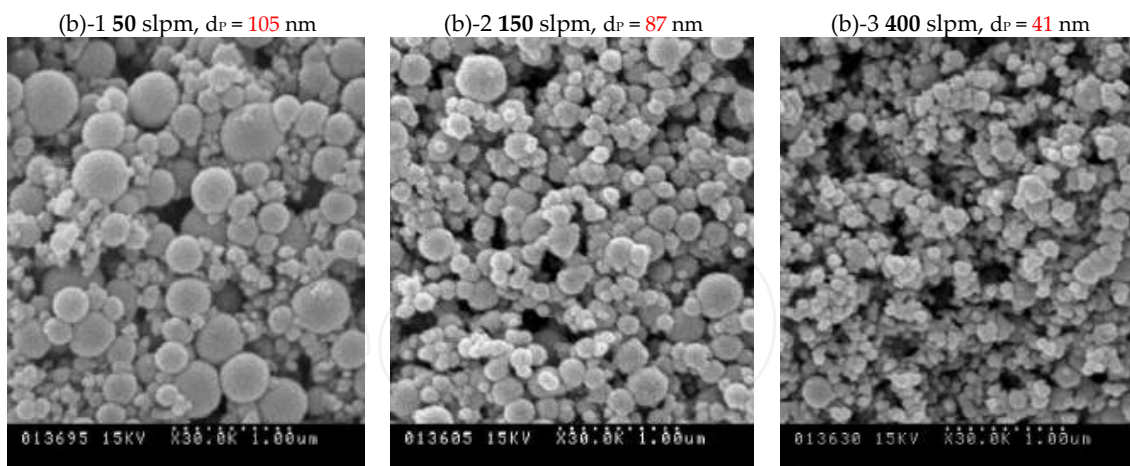
The particle size and distribution of nanopowders synthesized depend on both the evaporation of the feedstock and the quench of the vapour formed, which can be controlled by a number of plasma processing parameters. In the case of solid particle injected into the plasma, the nanopowders obtained could have included large micrometric particles if the feedstock was not completely vaporized in the plasma. If the required quench condition is not present, the nanoparticles formed could grow and agglomerate into large particles. The cooling rate of the gaseous product can determine both the particle sizes and their distributions. As the temperatures decrease, vapor condenses to liquid droplets and then solidifies to nanoparticles. According to the equation by Guo et al.,[6] the diameter of the droplets (d_p) is predominantly determined by the degree of supersaturation of vapor (S_v). The greater the S_v , the smaller the d_p . The S_v , on the other hand, is inversely proportional to the temperature T . The lower the T , the greater the S_v . Therefore, the cooling rate of vapor has to be extremely fast to obtain ultra

fine nanometric particles. Such a high-quench rate is usually achieved through proper design of reactor and injection of large amount of cooling gas, resulting in a typical cooling rate in the range of 10^5 to 10^6 K/s or higher.

Figure 15(a) shows an example that the particle size of germanium dioxide was a function of the quench gas flow rate used. The GeO_2 was synthesized from injection of germanium tetrachloride (GeCl_4) into oxygen plasma. The micrographs of the corresponding powders produced are shown in Figure 15(b-1–3), respectively. Figure 16 shows that different particle sizes and morphologies can also be obtained by altering quench and plasma operating conditions in the evaporation–recondensation of solid precursors.



(a) Particle size as a function of quench gas flow rate.



(b) SEM of the germanium oxide (GeO_2) particles produced from (GeCl_4+O_2) with different quench rates.

Figure 15. Effects of gas quench rates on the morphology and particle size of the nanopowders synthesized – liquid precursor

In the case of chemical reaction involved in the evaporation–condensation process, the control of quench rate is more delicate. Sufficiently high temperatures should be maintained in order for the reaction to complete before quench is introduced.

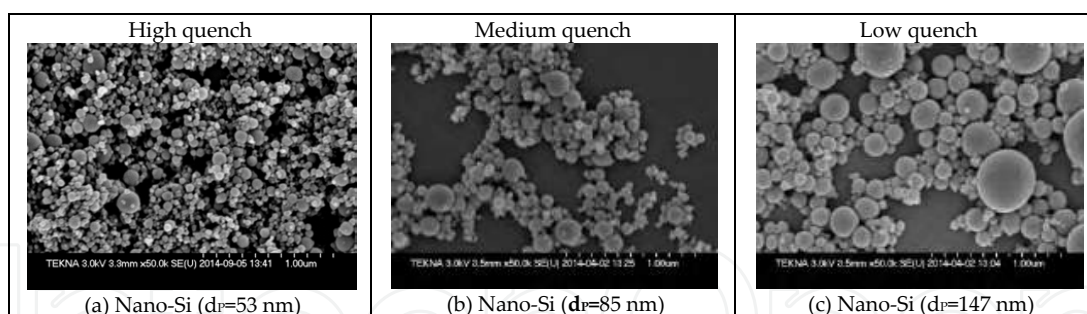


Figure 16. Effects of quench conditions on the morphology and particle size of the nanopowders synthesized – solid precursor

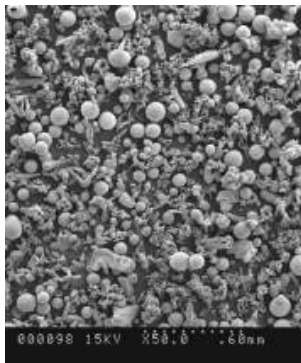
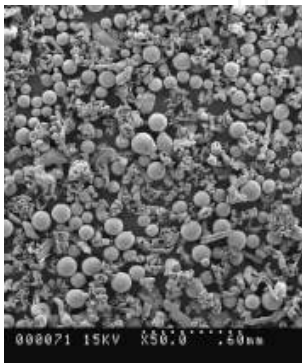
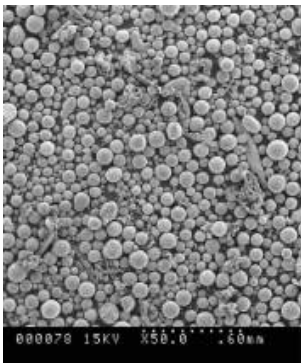
4.2. Chemical composition

In the synthesis of nanomaterials other than pure metals, there will be always some reactions involved during the plasma process. It remains a big challenge to ensure the completeness of desired reaction or to avoid the occurrence of undesired reaction under plasma conditions. Whether it is synthesis of oxide from oxidation of solid particles or synthesis of carbide or nitride from carburation or nitridation of condensed phases, undesired by-products or impurities could be present in the product powders. Obtaining a satisfactory purity or chemical composition of the product powder will require not only the optimization of the plasma processing parameters but very often a proper process and reactor design as well. As example, in the process of synthesis of nanometric CuO the product powders obtained may contain both CuO and Cu₂O phases.[6] To obtain pure CuO phase, certain measures had been taken, which include changing raw powder and its feeding conditions, modifying reactor structure to extend the high-temperature profile, and optimizing the plasma operating conditions. In the process of B₄C synthesis, the as-produced B₄C nanomaterials could contain free B, free C, and even some boron oxide.[6] These impurities came from different sources: free B was due to incomplete conversion of the B-containing precursor used; free C could be due to either incomplete reaction or excessive injection of the C-containing reacting agent; and the B₂O₃ could be due to oxidation of the unreacted B-containing precursor or the nanosized B₄C powders synthesized. It is not unlikely that nano-B₄C could be sensitive to air, and thus special care is needed for the handling of such powders after synthesis.

4.3. Processing efficiency

Induction plasma offers a simple tool for nanomaterial synthesis. Its efficiency, to a great extent, relies on the in-flight vaporization of fed materials in the high-temperature plasma. In order for the materials to be heated up sufficiently to evaporation, the fed materials should be all exposed to the high-temperature plasma. The evaporation rate of the fed materials often determines the production rate of the desired nanomaterial. In the case of particle injection, it was observed that the evaporation rate was closely related to the dispersion of fed particles in the plasma zones. When the powders are injected into plasma using a column-like pattern, some particles in the axial direction could not get adequate heating before being carried away from plasma zone. Poor dispersion greatly limits the process efficiency and the productivity

of the nanomaterial. A good dispersion allows for full utilization of the plasma energy at higher throughputs and thus results in higher production rate. Consequently, efforts should be made to improve the design of particle injector and to optimize the particle injection conditions. As examples, Figure 17 shows the comparison of powder dispersion patterns of three different types of particle injectors: Figure 17(a) pattern has minimal dispersion; Figure 17(b) pattern has limited dispersion; and Figure 17(c) pattern provides much improved dispersion. It can be anticipated that the energy utilization efficiency and powder productivity will increase as the dispersion is improved. To quantify the effect of the different types of injectors on the powder processing efficiencies, tests of spheroidization of Ti and Mo powders were carried out at Tekna's 60 kW induction plasma system. Spheroidization of Ti and Mo powders requires the particles injected into the plasma to be heated up to above 1668°C and 2623°C, respectively, for melting, followed by solidification. The raw powders were introduced into plasma using different injection probes at the same feed rate. After plasma treatment, the collected powders were evaluated by spheroidization efficiency or by measurement of tap density. The comparative test results for both Ti and Mo spheroidization are given in Table 4, showing that the Ti powder spheroidization efficiency was only 20% and 31%, respectively, with the powder injections shown in Figure 17(a) and (b). Significant increase in spheroidization was achieved with the much improved injection shown in Fig. 17(c), as the efficiency reached 90% under the same operating conditions. In the case of Mo spheroidization, the same trend was observed. The SEM micrographs reveal many more spherical particles obtained with injector 3 than with injector 1, as shown in Table 4. Higher spheroidization arised from better melting and densification of the particles. Therefore, the tap density of the Mo powders increased from 2.613 g/cm³ for raw to 4.582 g/cm³ after plasma treatment with the poor dispersion straight injection and also increased to 6.555 g/cm³ with the well-dispersed powder injection. Based on these results, one can expect similar effect in the processes of nanomaterial synthesis. The difference lies in that in the latter case, the dispersed particles must be heated up to boiling temperatures in plasma for being completely evaporated.

Powder type and feed rate	Spheroidization efficiency		
	Injector 1	Injector 2	Injector 3
	20%	31%	90%
(Ti, -100 mesh) 9,6 kg/hr			

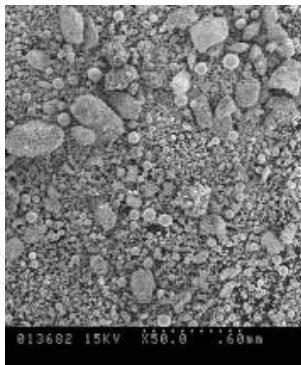
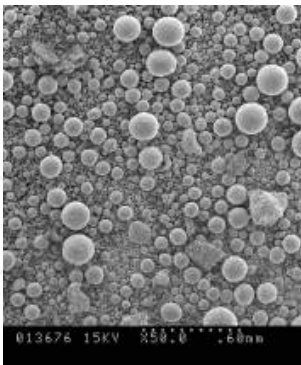
Powder type and feed rate	Spheroidization efficiency		
	Injector 1	Injector 2	Injector 3
(Mo, 10 - 400 μm ; Tap density = 2,613 g/cm^3 6 kg/hr	 <p>Tap density = 4,582 g/cm^3</p>		 <p>Tap density = 6,555 g/cm^3</p>

Table 4. Comparison of probe injectors vs. powder spheroidization efficiency

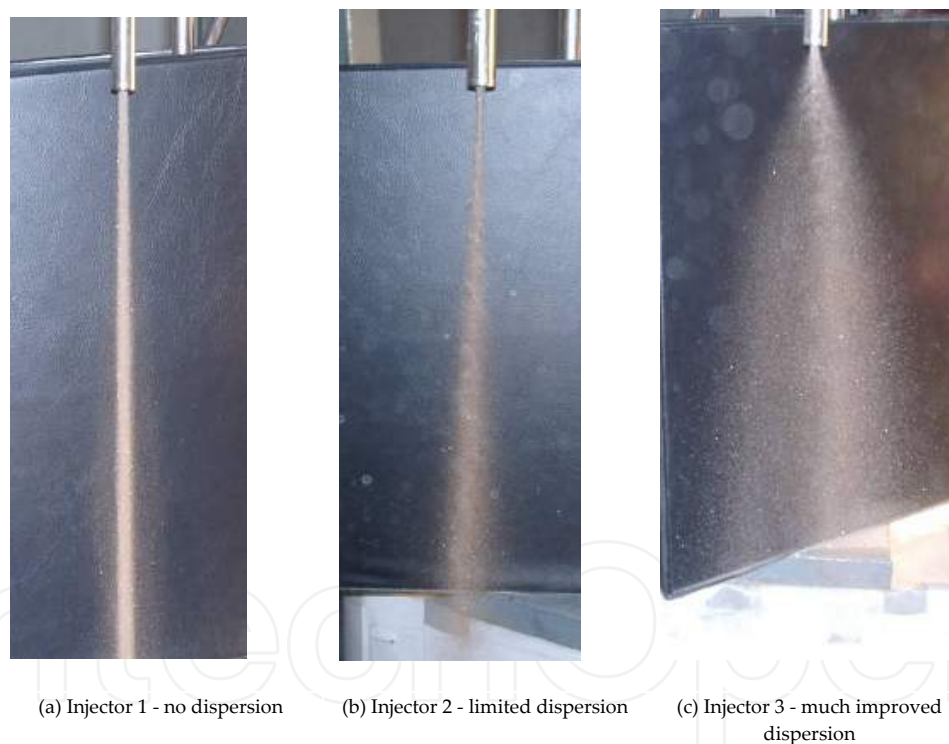


Figure 17. Particle dispersion patterns vs. probe design and injection conditions.

5. Summary and conclusion

Various nanomaterials have been successfully produced using Tekna’s induction plasma systems. The production rates and product compositions depend on the type of precursor,

reaction route, feeding conditions, plasma power level, and other processing parameters used. An improved dispersion of the fed materials in the plasma can significantly increase the productivity of the nanomaterials synthesized under the same operating conditions. Numerous quench methods and designs can be employed to control the particle sizes and the surface of the nanopowders produced. More developmental work will be required in the aspects of passivation and handling of reactive nanomaterials and classification and separation of the nanoparticles as-synthesized. Compared to the alternative techniques, induction plasma used for nanomaterial synthesis has the advantages of high purity, high versatility, scalability, and good controllability. It can be used in both laboratory and industrial scales.

Author details

Jiayin Guo*

Address all correspondence to: jiayin.guo@tekna.com

Tekna Plasma Systems Inc., Sherbrooke, Quebec, Canada

References

- [1] G. Beaucage, J.E. Mark, G. Burns, Wu H. Duen (editors), Nanostructured powders and their industrial applications, Materials Research Society Symposium Proceedings, Volume 520, San Francisco, CA, 13–15 April 1998.
- [2] K.-H. Cho, J.-E. Park, T. Osaka, S.-G. Park, The study of antimicrobial activity and preservative effects of nanosilver ingredient, *Electrochimica Acta*, Volume 51, Issue 5, Pages 956-960, 10 November 2005.
- [3] Electronics.ca Publications, “Nanomaterials and Markets to 2015,” Research Report INT6571, Technology Transfer Centre, Pages 245, 2008.
- [4] BCC Research Report NAN031E, “Nanotechnology: A realistic market assessment,” September 2012.
- [5] BCC Research Report AVM091A, Andrew McWilliams, “Emerging inkjet printing technologies, applications and global markets,” April 2013.
- [6] J. Guo, X. Fan, R. Dolbec, S. Xue, J. Jurewicz, M. Boulos, Development of nano-powder synthesis using inductive plasma, *Plasma Science and Technology*, Volume 12, Issue 2, Pages 188–199, April 2010.
- [7] V. Colombo, E. Ghedini, M. Gherardi, P. Sanibondi, Evaluation of precursor evaporation in Si nanoparticle synthesis by inductively coupled thermal plasmas, *Plasma*

- Sources Science and Technology, Volume 22, Issue 3, article id. 035010, Pages 1-11, 2013.
- [8] V. Colombo, E. Ghedini, P. Sanibondi, Three-dimensional investigation of particle treatment in an RF thermal plasma with reaction chamber, Plasma Sources Science and Technology, Volume 19, Issue 6, article id. 065024, Pages 1-13, 2010.
- [9] Jun-Ho Seo, Mi-Yeon Lee, Jeong-Soo Kim, Radio-frequency thermal plasma preparation of nano-sized Ni catalysts supported on MgO nano-rods for partial oxidation of methane, Surface and Coatings Technology, Volume 228, Supplement 1, Pages S91–S96, 15 August 2013.
- [10] Mi-Yeon Lee, Jeong-Soo Kim, Jun-Ho Seo, Radio-frequency thermal plasma synthesis of nano-sized indium zinc tin oxide powders with reduced indium content, Thin Solid Films, Volume 521, Pages 60–64, 30 October 2012.
- [11] Szilvia Klébert, Anna Mária Keszler, István Sajó, Eszter Drotár, Imre Bertóti, Eszter Bódis, Péter Fazekas, Zoltán Károly, János Szépvölgyi, Effect of the solid precursors on the formation of nanosized TiB_x powders in RF thermal plasma, Ceramics International, Volume 40, Issue 3, Pages 3925–3931, April 2014.
- [12] Audrone Jankeviciute, Zoltán Károly, Nadezda V. Tarakina, János Szépvölgyi, Aivaras Kareiva, Synthesis and characterization of spherical amorphous aluminosilicate nanoparticles using RF thermal plasma method, Journal of Non-Crystalline Solids, Volume 359, Pages 9–14, 1 January 2013.
- [13] Z. Károly, I. Mohai, S. Klébert, A. Keszler, I.E. Sajó, J. Szépvölgyi, Synthesis of SiC powder by RF plasma technique, Powder Technology, Volume 214, Issue 3, Pages 300–305, 25 December 2011.
- [14] G. Çakmak, Z. Károly, I. Mohai, T. Öztürk, J. Szépvölgyi, The processing of Mg–Ti for hydrogen storage; mechanical milling and plasma synthesis, International Journal of Hydrogen Energy, Volume 35, Issue 19, Pages 10,412–10,418, October 2010.
- [15] B. Aktekin, G. Çakmak, T. Öztürk, Induction thermal plasma synthesis of Mg₂Ni nanoparticles, International Journal of Hydrogen Energy, Volume 39, Issue 18, Pages 9859–9864, 15 June 2014.
- [16] János Szépvölgyi, Ilona Mohai, Zoltán Károly, Loránd Gál, Synthesis of nanosized ceramic powders in a radiofrequency thermal plasma reactor, Journal of the European Ceramic Society, Volume 27, Issues 2–3, Pages 941–945, 2008.
- [17] Ilona Mohai, Loránd Gál, János Szépvölgyi, Jenő Gubicza, Zsuzsa Farkas, Synthesis of nanosized zinc ferrite from liquid precursors in RF thermal plasma reactor, Journal of the European Ceramic Society, Volume 27, Issues 2–3, Pages 941–945, 2007.
- [18] R. Kumara, K.H. Prakash, P. Cheanga, K.A. Khorb, Microstructure and mechanical properties of spark plasma sintered zirconia-hydroxyapatite nano-composite powders, Acta Materialia, Volume 53, Issue 8, Pages 2327–2335, May 2005.

- [19] Rajendra Kumara, P. Cheanga, K.A. Khorb, Radio frequency (RF) suspension plasma sprayed ultra-fine hydroxyapatite (HA)/zirconia composite powders, *Biomaterials*, Volume 24, Issue 15, Pages 2611–2621, July 2003.
- [20] Ji-Guang Li, Takamasa Ishigaki, One-step Ar/O₂ thermal plasma processing of Y₂O₃:Eu³⁺ red phosphors: Phase structure, photoluminescent properties, and the effects of Sc³⁺ codoping, *Journal of Solid State Chemistry*, Volume 196, Pages 58–62, December 2012.
- [21] Chenning Zhang, Masashi Ikeda, Masaaki Isobe, Tetsuo Uchikoshi, Ji-Guang Li, Takayuki Watanabe, Takamasa Ishigaki, Phase composition and magnetic properties of niobium–iron codoped TiO₂ nanoparticles synthesized in Ar/O₂ radio-frequency thermal plasma, *Journal of Solid State Chemistry*, Volume 184, Issue 9, Pages 2525–2532, September 2011.
- [22] C.-N. Zhang, J.-G. Li, Y.-H. Leng, T. Uchikoshi, T. Watanabe, T. Ishigaki, (Eu³⁺–Nb⁵⁺)-codoped TiO₂ nanopowders synthesized via Ar/O₂ radio frequency thermal plasma oxidation processing: Phase composition and photoluminescence, *Thin Solid Films*, Volume 518, Issue 13, Pages 3531–3534, 30 April 2010.
- [23] J.-G. Li, M. Ikeda, R. Ye, Y. Moriyoshi, T. Ishigaki, Control of particle size and phase formation of TiO₂ nanoparticles synthesized in RF induction plasma, *Journal of Physics D: Applied Physics*, Volume 40, Pages 2348, 2007.
- [24] Toshitaka Nakamura, Hironaka Fujii, Hiroaki Miyagawa, Rajesh Mukherjee, Bin Zhang, Amane Mochizuki, Light emitting device with translucent ceramic plate, United States Patent 8502442, 08 June 2013.
- [25] Hiroaki Miyagawa, Toshitaka Nakamura, Hironaka Fujii, Amane Mochizuki, Method of manufacturing phosphor translucent ceramics and light emitting devices, United States Patent 8298442, 30-10-2012.
- [26] Rajesh Mukherjee, Toshitaka Nakamura, Sheng Li, Brett T. Harding, Amane Mochizuki, Production of phase-pure ceramic garnet particles, United States Patent 8206672, 26-06-2012.
- [27] Keun Su Kim, Ala Moradian, Javad Mostaghimi, Yasaman Alinejad, Ali Shahverdi, Benoit Simard, Gervais Soucy, Synthesis of single-walled carbon nanotubes by induction thermal plasma, *Nano Research*, Volume 2, Pages 817670, 2009.
- [28] Keun Su Kim, German Cota-Sanchez¹, Christopher T. Kingston, Matej Imris, Benoit Simard, Gervais Soucy, Large-scale production of single-walled carbon nanotubes by induction thermal plasma, *Journal of Physics D: Applied Physics*, Volume 40, Pages 2375–2387, 2007.
- [29] Benoit Simard, Christopher Thomas Kingston, Stephane Denommee, Gervais Soucy, German Cota-sanchez, Method and apparatus for the continuous production and

functionalization of single-walled carbon nanotubes using a high frequency plasma torch, EP20060705309, 2013-07-08.

- [30] Ali Shahverdi, Gervais Soucy, Benoit Simard, Javad Mostaghimi, Effect of ammonia gas addition to the synthesis environment of single-walled carbon nanotubes on their surface chemistry, *Chemical Engineering Journal*, Volume 230, Pages 80–92, October 2013.
- [31] I.A. Castillo, R.J. Munz, Transient heat, mass and momentum transfer of an evaporating stationary droplet containing dissolved cerium nitrate in a RF thermal argon-oxygen plasma under reduced pressure, *International Journal of Heat and Mass Transfer*, Volume 50, Pages 240–256, 2007.
- [32] I.A. Castillo, R.J. Munz, New in-situ sampling and analysis of the production of CeO₂ powders from liquid precursors using a novel wet collection system in a RF inductively coupled thermal plasma reactor. Part 1: Reactor system and sampling probe, *Plasma Chemistry and Plasma Processing*, Volume 27, Issue 6, Pages 737–759, 2007.
- [33] I.A. Castillo, R.J. Munz, New in-situ sampling and analysis of the production of CeO₂ powders from liquid precursors in a RF thermal plasma reactor. Part 2: Analysis of CeO₂ powders, fuel addition and image analysis, *Plasma Chemistry and Plasma Processing*, Volume 27, Issue 6, Pages 761–788, 2007.
- [34] Ian A. Castillo, Richard J. Munz, Inductively coupled plasma synthesis of CeO₂-based powders from liquid solutions for SOFC electrolytes, *Plasma Chemistry and Plasma Processing*, Volume 25, Issue 2, April 2005.
- [35] D. Harbec, F. Gitzhofer, A. Tagnit-Hamou, Induction plasma synthesis of nanometric spheroidized glass powder for use in cementitious materials, *Powder Technology*, Volume 214, Issue 3, Pages 356–364, 2011.
- [36] Behnam Mostajeran Goortani, Pierre Proulx, Siwen Xue, Norma Y. Mendoza-Gonzalez, Controlling nanostructure in thermal plasma processing: Moving from highly aggregated porous structure to spherical silica nanoparticles, *Powder Technology*, Volume 175, Issue 1, Pages 22–32, 2007.
- [37] Gary A. Fielding, Mangal Roy, Amit Bandyopadhyay, Susmita Bose, Antibacterial and biological characteristics of silver containing and strontium doped plasma sprayed hydroxyapatite coatings, *Acta Biomaterialia*, Volume 8, Issue 8, Pages 3144–3152, August 2012.
- [38] Mangal Roy, Vamsi Krishna Balla, Amit Bandyopadhyay, Susmita Bose, Compositionally graded hydroxyapatite/tricalcium phosphate coating on Ti by laser and induction plasma, *Acta Biomaterialia*, Volume 7, Issue 2, Pages 866–873, February 2011.
- [39] Mangal Roy, Amit Bandyopadhyay, Susmita Bose, Induction plasma sprayed nano hydroxyapatite coatings on titanium for orthopaedic and dental implants, *Surface and Coatings Technology*, Volume 205, Issues 8–9, Pages 2785–2792, 25 January 2011.

- [40] Chopra NG, Luyken RJ, Cherrey K, Crespi VH, Cohen ML, Louie SG, Zettl A., Boron nitride nanotubes, *Science*, Volume 269, Issue 5226, Pages 966-967, 1995.
- [41] K.H. Khoo, M.S. Mazzoni, Steven G. Louie, Tuning the electronic properties of boron nitride nanotubes with transverse electric fields: A giant dc Stark effect, *Physical Review B*, Volume 69, Issue 20, ID 201401, 2004.
- [42] Masa Ishigami, Shaul Aloni, A. Zettl, University of California at Berkeley, CP696, *Scanning Tunneling Microscopy/Spectroscopy and Related Techniques: 12th International Conference*, edited by P.M. Koenraad, M. Kemerink, 2003.
- [43] Chunyi Zhi, Yoshio Bando, Chengchun Tang, Dmitri Golberg, Boron nitride nanotubes, *Materials Science and Engineering: R: Reports*, Volume 70, Issues 3–6, Pages 92–111, 22 November 2010, 3rd IEEE International NanoElectronics Conference (IN-EC).
- [44] Michael W. Smith, Kevin Jordan, Cheol Park, Boron nitride nanotubes, USPTO Patent Application 20090117021.
- [45] Chris Kingston, Large-scale synthesis of few-walled small diameter boron nitride nanotubes (sub-10 nm) by an induction thermal plasma. National Research Council Canada, NT13, Espoo Finland, 28 June 2013.
- [46] Michael W. Smith, Kevin C. Jordan, Jonathan C. Stevens, Induction – coupled plasma synthesis of boron nitride nanotubes, USPTO Application 20150125374.
- [47] Jiayin Guo, Preliminary trials of 15 kW ICP unit for synthesis of boron nitride nanotubes (BNNT), Tekna internal R & D report, 2015.
- [48] M. Rahmane, G. Soucy, M.I. Boulos, Mass transfer in induction plasma reactors, part 2, radial injection mode, *International Journal of Heat Mass Transfer*, Volume 37, Issue 14, Pages 2035-2046, 1994.
- [49] M.I. Boulos, P. Fauchais, E. Pfender, *Thermal plasmas: Fundamentals and applications*, Volume 1, New York, Plenum Press, 1994.
- [50] Jiayin Guo, Study on production of ultrafine aluminum powders using induction plasmas, Tekna internal R & D report, 8 June 2000.
- [51] Jiayin Guo, Synthesis of nanometric aluminum powders – field trials (1), Tekna internal R & D report, 28 December 2007.
- [52] Jiayin Guo, Synthesis of nanometric aluminum powders – field trials (2), Tekna internal R & D report, 18 July 2008.
- [53] Jiayin Guo, Synthesis of silver UFP by induction plasma at System 28B, Tekna internal R & D report, 27 June 2003.
- [54] Jiayin Guo, Synthesis of nanometric nickel powders using induction plasma, Tekna internal R & D report, October 2003.

- [55] Jiayin Guo, Synthesis of nanometric Ni powders from nickel carbonyl using induction plasma – 1st campaign, Tekna internal R & D report, 17 November 2004.
- [56] Jiayin Guo, Synthesis of nanometric Ni powders from nickel carbonyl using induction plasma – 3rd campaign, Tekna internal R & D report, 11 May 2005.
- [57] Jiayin Guo, Production of nanometric Ni sample powders with desired particle sizes, Tekna internal R & D report, 20 March 2008.
- [58] Jiayin Guo, Synthesis of nanometric boron and boron carbide powders using induction plasma, Tekna internal R & D report, 15 March 2005.
- [59] Jiayin Guo, Induction plasma synthesis of nano-sized chromium powders, Tekna internal R & D report, 08 July 2013.
- [60] Jiayin Guo, Induction plasma synthesis of nano-sized copper powders, Tekna internal R & D report, 14 January 2014.
- [61] Jiayin Guo, Induction plasma synthesis of nanometric silicon powders, Tekna internal R & D report, 20 May 2012.
- [62] Jiayin Guo, Induction plasma synthesis of nano-sized silicon powders, Tekna internal R & D report, 31 May 2013.
- [63] Jiayin Guo, Induction plasma synthesis of nano-sized silicon powders with reduced oxygen content, Tekna internal R & D report, 01 April 2014.
- [64] Jiayin Guo, Start-up experimental trials of 15 kW ICP unit - synthesis of nano-sized silicon powders, Tekna internal R & D report, 18 March 2014.
- [65] Jiayin Guo, Synthesis of nanometric tungsten powders, Tekna internal R & D report, 11 February 2008.
- [66] Jiayin Guo, Induction plasma spheroidization of fine tungsten powders, Tekna internal R & D report, 06 September 2013.
- [67] Jiayin Guo, Production of ultrafine copper oxide powders using induction plasmas, Tekna internal R & D report, 30 March 2000.
- [68] Jiayin Guo, Production of molybdenum trioxide UFP by HF plasma at System 6, Tekna internal R & D report, 21 February 2002.
- [69] Jiayin Guo, Induction plasma synthesis of nanometric indium-tin oxide composite powders, Tekna internal R & D report, 12 November 2003.
- [70] Jiayin Guo, Induction plasma synthesis of nanometric indium-tin oxide composite powders (2), Tekna internal R & D report, 05 February 2004.
- [71] Jiayin Guo, Synthesis of nanometric yttrium oxide powders by induction plasma decomposition of oxalate, Tekna internal R & D report, 03 November 2004.

- [72] Jiayin Guo, "Synthesis of nanometric yttrium oxide powders by induction plasma – 3rd campaign, Tekna internal R & D report, 13 January 2006.
- [73] Jiayin Guo, Synthesis of nanometric silicon monoxide (SiO) powders through hydrogen reduction of silica (SiO₂) in induction plasma, Tekna internal R & D report, 16 December 2004.
- [74] Jiayin Guo, Synthesis of nanometric composite ceramic powders (ZrO₂+La₂O₃+Al₂O₃) using induction plasma, Tekna internal R & D report, 20 July 2005.
- [75] Jiayin Guo, Synthesis of nanometric cerium oxide powders using induction plasma – preliminary trials, Tekna internal R & D report, 16 November 2006.
- [76] Jiayin Guo, Synthesis of nanometric glass powders from coarse (xAl₂O₃+ySiO₂+zMgO) mixture using induction plasma, Tekna internal R & D report, 04 July 2006.
- [77] Jiayin Guo, Synthesis of nanometric glass powders using induction plasma – preliminary trials, Tekna internal R & D report, 14 September 2006.
- [78] Jiayin Guo, Synthesis of nanometric glass powders using induction plasma – production of 2 kg sample, Tekna internal R & D report, 16 October 2006.
- [79] Jiayin Guo, Synthesis of nanometric glass powders using induction plasma – Sy51 validation trials, Tekna internal R & D report, 20 February 2007.
- [80] Jiayin Guo, Induction plasma synthesis of nano-sized borosilicate-based glass powders, Tekna internal R & D report, 15 August 2013.
- [81] Jiayin Guo, Induction plasma synthesis of nano-sized PbO-based glass powders, Tekna internal R & D report, 16 November 2012.
- [82] Jiayin Guo, Induction plasma synthesis of nano-sized PbO-based glass powders, Tekna internal R & D report, 10 April 2013.
- [83] Jiayin Guo, Induction plasma synthesis of nano-sized gadolinium zirconate (Gd₂Zr₂O₇) powders, Tekna internal R & D report, 14 January 2013.
- [84] Jiayin Guo, Induction plasma synthesis of nano-sized gadolinium zirconate (Gd₂Zr₂O₇) powders (2), Tekna internal R & D report, 26 September 2013.
- [85] Jiayin Guo, Start-up experimental trials of 15 kW ICP unit - synthesis of nano-sized powders, Tekna internal R & D report, 18 March 2014.
- [86] Jiayin Guo, Induction plasma synthesis of nano-sized SiO₂ powders, Tekna internal R & D report, 30 April 2013.
- [87] Jiayin Guo, Induction plasma synthesis of nano-sized silicon dioxide powders, Tekna internal R & D report, 04 July 2013.

- [88] Jiayin Guo, Induction plasma synthesis of nano-sized titanium dioxide powders, Tekna internal R & D report, 18 July 2014.
- [89] Jiayin Guo, Induction plasma synthesis of nano-sized aluminium oxide powders, Tekna internal R & D report, 29 May 2015.
- [90] Jiayin Guo, Induction plasma synthesis of nanometric B₄C powders from (BCl₃ + CH₄) system – preliminary trials, Tekna internal R & D report, 18 January 2007.
- [91] Jiayin Guo, Induction plasma synthesis of nanometric B₄C powders from (BCl₃ + CH₄) system – process optimization, Tekna internal R & D report, 21 March 2007.
- [92] Jiayin Guo, Induction plasma synthesis of nanometric silicon carbide powders, Tekna internal R & D report, 31 August 2012.
- [93] Jiayin Guo, Induction plasma synthesis of nanometric silicon carbide powders, Tekna internal R & D report, 26 November 2012.
- [94] Jiayin Guo, Induction plasma synthesis of nano-sized zinc sulfide powders – 2014 campaign, Tekna internal R & D report, 12 June 2014.
- [95] Jiayin Guo, Preliminary trials of preparation of carbon nanotubes by induction plasma technology, Tekna internal R & D report, 21 November 2000.
- [96] Jiayin Guo, Demonstration trials of 15 kW ICP unit for synthesis of SiO nanowires, Tekna internal R & D report, 31 May 2015.